Impact of the amino acid sequence on the conformation of side chain lactam-bridged octapeptides

Saskia Neukirchen,[a,b] Viktoria Krieger,[b,c] Cornelia Roschger,[a] Mario Schubert,[a] Brigitta Elsässer[a] and Chiara Cabrele[a]* ⓘ

Synthetic helical peptides are valuable scaffolds for the development of modulators of protein–protein interactions involving helical motifs. Backbone-to-side chain or side chain-to-side chain constraints have been and still are intensively exploited to stabilize short α-helices. Very often, these constraints have been combined with backbone modifications induced by Cα-tetrasubstituted, β-, or γ-amino acids, which facilitate the α-peptide or $\alpha/\beta/\gamma$-peptide adopting an α-helical conformation. In this work, we investigated the helical character of octapeptides that were cyclized by a Lys-Asp-$(i,i+4)$-lactam bridge. We started with two sequences extracted from the helix–loop–helix region of the Id proteins, which are inhibitors of cell differentiation during development and in cancer. Nineteen analogs containing the lactam bridge at different positions and displaying different amino acid core triads $(i+1,2,3)$ as well as outer residues were prepared by solid-phase methodology. Their conformation in water and water/2,2,2-trifluoroethanol mixtures was investigated by circular dichroism (CD) spectroscopy. The cyclopeptides could be grouped in helix-prone and non-helix-prone structures. Both the amino acid core triad $(i+1,2,3)$ and the pendant residues positively or negatively affected the formation of a helical structure. Computational studies based on the NMR-derived helical structure of a cyclopeptide containing Aib at position $(i+2)$ of the triad were generally in agreement with the secondary structure propensity of the cyclopeptides observed by CD spectroscopy. In conclusion, the Lys-Asp-$(i,i+4)$-lactam bridge may succeed or fail in the stabilization of short helices, depending on the primary structure. Moreover, computational methods may be valuable tools to discriminate helix-prone from non-helix-prone peptide-based macrolactams. Copyright © 2017 European Peptide Society and John Wiley & Sons, Ltd.

Additional Supporting Information may be found online in the supporting information tab for this article.

Keywords: cyclopeptides; lactam bridge; side chain cyclization; circular dichroism; computational methods; modeling; molecular dynamics; NMR spectroscopy

Introduction

Protein–protein interactions are key events in cellular signaling and cover a highly important area of research aiming at their detection and modulation *in vitro* and *in vivo* [1,2]. As the α-helix is the most common secondary structure found in proteins, it plays a key role in molecular recognition. Therefore, many efforts are made to mimic interacting α-helices and use them for the modulation of protein interactions involving α-helices [3–11]. Several approaches can be used to stabilize the helical conformation of a short peptide sequence: Some of these are based on metal ion chelation [12,13], helix-nucleating templates [14–16], hydrogen bond surrogates [17,18], non-covalent side chain constraints [19,20] and covalent side chain linkages such as the disulfide [21], thioether [22,23], triazole [24,25], hydrocarbon [7,9,10,26–28], diester [29], and lactam bridges [30–38]. Alternatively or in combination with covalent constraints, unnatural amino acids with preference for the helical structure can be used, like Cα-tetrasubstituted, β-, and γ-amino acids [4,5,28,29,39].

One of the simplest methods to stabilize the helical conformation is the introduction of a side chain lactam bridge upon the covalent linkage of the proteinogenic residues Lys and Asp/Glu [40–42]. These residues should be located at positions $(i,i+3)$ or $(i,$ $i+4)$, in order to stabilize a 3_{10}-helical or α-helical turn, respectively. Accordingly, Fairlie and coworkers reported on Lys-Asp-$(i,i+4)$-lactam-bridged pentapeptides and hexapeptides that adopted such a motif in water [35]. Instead, the $(i,i+7)$ linkage should be suitable to stabilize two α-helical turns, but it requires a bridge longer than seven or eight atoms, which makes it necessary to insert additional linkers (e.g. Ala or β-Ala residues) or to use artificial building blocks such as Dap(AMPA = 4-(aminomethyl)phenylacetic acid) in place of Lys [37].

We are interested in the development of peptide-based modulators of the Id proteins that are members of the large family

* Correspondence to: Chiara Cabrele, Department of Molecular Biology, University of Salzburg, Billrothstrasse 11, 5020 Salzburg, Austria. E-mail: chiara.cabrele@sbg.ac.at

a Department of Molecular Biology, University of Salzburg, Billrothstrasse 11, 5020, Salzburg, Austria

b Faculty of Chemistry and Biochemistry, Ruhr University Bochum, Universitätsstrasse 150, 44801, Bochum, Germany

c Institute of Pharmaceutical and Medicinal Chemistry, Heinrich Heine University Düsseldorf, Universitätsstrasse 1, 40225, Düsseldorf, Germany

of the helix–loop–helix (HLH) transcription factors and play an important role in fetal development as well as in cancer [43–46]. Their mode of action is based on specific protein–protein interactions with basic HLH (bHLH) transcription factors like the E proteins (e.g. E47) and the muscle regulatory factors (e.g. MyoD) [47–49]. The resulting Id/bHLH heterodimers are unable to bind the DNA (contrarily to bHLH/bHLH dimers), thus blocking bHLH-mediated DNA transcription. Such inhibitory activity allows the cells staying in an undifferentiated state, proliferating, migrating, and delaying senescence [50,51]. Because the Id proteins are upregulated in several cancer types while being downregulated in healthy adult cells, they are interesting molecular targets for cancer therapy [52,53].

Short fragments from the MyoD or Id HLH domains have been reported to interact with the Id proteins and modulate their function in cells [54,55]. By using a fragment scan approach, we recently showed that octapeptides reproducing part of either helix or helix–loop junction of the Id HLH domain are able to recognize the Id HLH domain itself in the low micromolar range [56]. Here, we present a synthetic and structural study with the aim to evaluate the effect of a Lys-Asp-($i,i + 4$)-lactam bridge on octapeptides extracted from the Id HLH domain. We chose the two helix–loop junctions as octapeptide scaffolds (junction-1: SR(/K)LR(/K)ELVP, and junction-2: L(/V)SQ(/K)V(/M)EILQ [57,58], as these regions are highly conserved within the Id1–4 proteins (Figure 1) and are important for the correct folding of the Id protein HLH domain into helical bundles [59–61].

We designed and synthesized 19 Lys-Asp-($i,i + 4$)-lactam-bridged octapeptides and investigated their conformation in water and water/TFE mixtures by CD spectroscopy (Table 1). Based on their CD signature, the cyclopeptides were classified in helix-prone and non-helix-prone structures. The effects of the position of the side chain constraint and of the residues inside and outside the macrocycle on the cyclopeptides conformation are discussed in the following sections. Briefly, the amino acid triad ($i + 1,2,3$) included in the macrolactam was found to affect the secondary structure propensity; in particular, amino acid residues commonly found in helices, or known to stabilize helices like 2-aminoisobutyric

Table 1. Amino acid sequence and dichroic properties of the synthesized cyclopeptides (B = Aib; Z = Nle)

Cyclopeptide no.	KD-($i,i + 4$)-lactam-bridged sequence[a]	CD band[b] $\pi \rightarrow \pi^*$ (nm)	CD band[b] $n \rightarrow \pi^*$ (nm)
1	**K**RL**KD**LVP	203/204	210–235
2	S**K**L**KED**VP	—	—
3	SR**KKELD**P	200/204	—
4	V**KKVED**LQ	194/197	223/224[c]
5	VS**K**VE**ID**Q	193/195	220/220
6	VS**KKEIL D**	—	—
7	SR**KKELD**A	208/207	218/218
8	SR**KK**LE**D**P	202/203	—
9	SR**KK**LE**D**A	210/206	222/220
10	V**K**RB**QD**LQ	206/209	223/219
11	V**K**RL**QD**LQ	205/206	218/222
12	V**K**RZ**QD**LQ	205/207	222/220
13	V**K**RW**QD**LQ	205/207	221/219
14	V**K**RV**QD**LQ	205/207	222/220
15	V**K**QL**QD**LQ	206/207	216/217
16	V**K**QZ**QD**LQ	206/207	218/221
17	V**K**QW**QD**LQ	203/206	219/218
18	V**KKELD**LQ	205/206	218/218
19	V**KKEVD**LQ	194/195	215/215[c]

[a]All cyclopeptides are N-terminally acetylated and C-terminally amidated. Bold residues are side chain cyclized.
[b]Position of the negative CD band in water without/with 30% TFE.
[c]Positive CD band.

acid (Aib) [39,62], favored the helical conformation. However, also the pendant positions influenced the type of CD signature of the cyclopetides: For example, a Pro or Ala residue at position ($i + 5$) gave a non-helix-like or helix-like CD signature, respectively. This suggests that the amino acid sequence plays a determinant role in the control and fine-tuning of the structure of the macrolactam, which may modulate the effect of the side chain constraint [35].
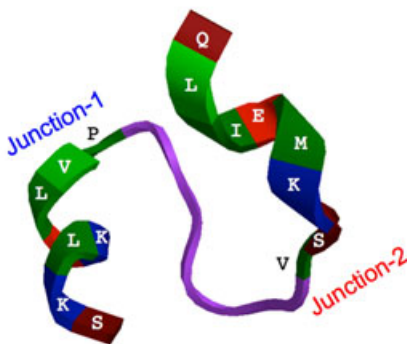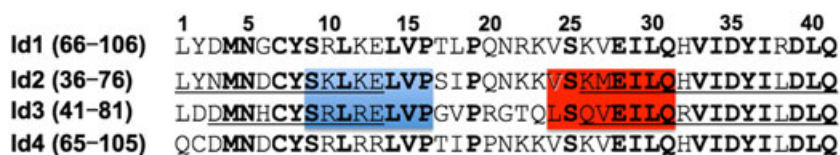

Figure 1. Amino acid sequence of the HLH domains of Id1–4 (top) and view of the crystal structure of the Id2 fragment 44–66 containing the helix–loop junctions (bottom, color code: green, brown, red, and blue for hydrophobic, polar uncharged, acidic, and basic residues, respectively). The helical regions found in the NMR structure of the Id3 HLH domain (PDB ID: 2LFH) [57] and in the crystal structure of the Id2 HLH domain (PDB ID: 4AYA) [58] are underlined. Junction-1 and junction-2 are in the blue and red boxes, respectively. The conserved residues within the Id family are in bold.

Materials and Methods

Materials

Chemical reagents and solvents for the peptide syntheses were of peptide synthesis grade; solvents for HPLC and spectroscopy were of HPLC or spectroscopy grade. Fmoc-protected amino acids, Rink Amide MBHA resins (100–200 mesh, loading 0.45–0.56 mmol/g), 2-(1*H*-benzotriazole-1-yl)-1,1,3,3-tetramethyluronium hexafluorophosphate (HBTU), *N,N*-diisopropylethylamine (DIPEA), piperidine, *N,N*-dimethylformamide (DMF), *N*-methyl-2-pyrrolidone (NMP), dichloromethane (DCM), diethyl ether, CH_3CN, and trifluoroacetic acid (TFA) were purchased from Novabiochem (Merck, Darmstadt, Germany), Biosolve (Valkenswaard, Netherland) and Iris Biotech (Marktredwitz, Germany). Triisopropylsilane (TIS), 1,2-ethanedithiol (EDT), thioanisole (TIA), *N*-hydroxybenzotriazole (HOBt), acetic anhydride, $PhSiH_3$, and $Pd(PPh_3)_4$ were purchased from Sigma-Aldrich (Munich, Germany). α-Cyano-4-hydroxycinnamic acid was purchased from Acros Organics (Geel, Belgium). D_2O was from Armar GmbH (Leipzig, Germany). Dulbecco's modified Eagle's medium – high glucose, fetal bovine serum (FBS), penicillin–streptomycin, 3-(4,5-dimethylthiazole-2-yl)-2,5-diphenyltetrazolium bromide (MTT), and dimethylsulfoxide (DMSO) were purchased from Sigma-Aldrich. The human breast cancer cell line T47D was a gift from the Paracelsus Medical University, Salzburg, Austria.

Methods

The solid-phase peptide syntheses were carried out on an automatic peptide synthesizer (Syro, Multisyntech, Witten, Germany, and Syro I, Biotage). The analytical and semipreparative HPLC equipment was from Agilent Technologies, Böblingen, Germany (1200 Series) and Thermo Fisher Scientific, Germering, Germany (Ultimate 3000). The analytical and semipreparative columns were from Macherey Nagel, Düren, Germany (Nucleosil C_{18}, 4 × 250 mm and 10 × 250 mm), Thermo Fisher Scientific (Syncronis C_{18}, 4.6 × 250 mm), and Merck (Chromolith RP-18e, 10 × 100 mm). The gradient used for analytical HPLC was the following: 3% B for 8 min, up to 60% B over 35 min (A = H_2O with 0.06% TFA; B = CH_3CN with 0.05% TFA). MALDI-TOF mass spectra were recorded on an Autoflex mass spectrometer from Bruker Daltonics (Bremen, Germany) using α-cyano-4-hydroxycinnamic acid as matrix. The CD measurements were recorded on a Jasco J-815 CD spectrometer. The UV measurements were carried out on a Varian Cary 1E UV–visible spectrophotometer. The absorption measurements for the MTT assay were carried out on a Tecan Infinite 200M Pro microplate reader. The NMR spectra were recorded on a Bruker BioSpin (Rheinstetten, Germany) AVANCE III HD 600-MHz spectrometer equipped with a QXI ($^1H/^{13}C/^{15}N/^{31}P$) probe. Structure optimization and molecular dynamics simulations were carried out using MOE2015.10 [63] (Amber 99 force field). Stepwise molecular dynamics calculations were performed by using NWChem 6.6 [64].

Peptide synthesis

The linear peptides were assembled on an automatic peptide synthesizer by using a Rink Amide resin and Fmoc chemistry. The side chain protecting groups were *t*-Bu (Ser, Asp, Glu), Boc (Lys, Trp), Alloc (Lys to be cyclized), allyl (Asp to be cyclized), and Pbf (Arg). The Fmoc deprotection was carried out with 28% piperidine in DMF/NMP (70:30, *v/v*) for 3 min and 14% piperidine in DMF/NMP (70:30, *v/v*) for 10 min. The couplings were accomplished with the mixture Fmoc-AA-OH/HOBt/HBTU/DIPEA (5:5:4.8:10 equiv) for 2 × 40 min. N-terminal acetylation was performed manually with acetic anhydride/DIPEA (10:10 equiv) in DMF for 30 min. To control the quality of the linear peptide chain by HPLC and MS, a small portion of the peptidyl resin was treated with TFA/H_2O/TIA/EDT/TIS (80:5:5:5:5; V_{tot} = 100 µl) for about 2 h. Ice-cold diethyl ether was added to precipitate the peptide that was recovered by centrifugation and washed several times with ice-cold diethyl ether. The Alloc/allyl protecting groups were orthogonally removed by repeated treatments (6 × 20 min) with $Pd(PPh_3)_4$ (0.5 equiv) in the presence of $PhSiH_3$ (25 equiv) in DCM. Side chain cyclization was carried out with DIPEA/3-(diethoxyphosphoryloxy)-1,2,3-benzotriazin-4(3H)-one (DEPBT) (3:2 equiv) in DCM/DMF (3:1, *v/v*) and monitored (generally over 72 h) by MS after small-scale TFA cleavage. The cyclization yielded different ratios of product/oligomer depending on the peptide sequence. The cyclized peptides were cleaved from the resin with TFA/H_2O/TIA/EDT/TIS (80:5:5:5:5; V_{tot} = 1 ml) for about 3 h, precipitated by ice-cold diethyl ether, and recovered by centrifugation at 3 °C for 5 min. The crude peptides were purified by semipreparative HPLC. The homogeneity (≥90%, except for cyclopeptide **7**, which was ~70% homogeneous) and identification of the desired cyclopeptides were assessed by analytical HPLC and MALDI-TOF-MS (Table S1 and Figures S1–S3). One-dimensional ^1H-NMR spectra of the synthetically more easily accessible cyclopeptides **5**, **10**–**18**, which were obtained in sufficient amount, were recorded in H_2O/D_2O (12:1, *v/v*) at 298 K by using excitation sculpting or 3-9-19 WATERGATE for the suppression of the water signal (Figure S4).

CD spectroscopy

The peptides were dissolved in water and a water/TFE mixture (70:30, *v/v*) at the following concentrations: 50 µM (**1**, **3**–**5**, **7**–**9**, **13**, **18**, **19**), 44 µM (**14**), 40 µM (**15**, **16**), 33 µM (**11**), 20 µM (**12**, **17**), and 15 µM (**10**). The CD spectra were recorded at 20 °C using a 1-mm quartz cell from Hellma Analytics. For each CD spectrum, four scans were accumulated using a step resolution of 0.1 nm, a bandwidth of 1 nm, and a response time of 2 s. The CD signal was recorded from 260 to 190 nm with a scan speed of 20 nm/min. The CD spectrum of the solvent was subtracted, and the difference spectrum was normalized to express the ellipticity in mean residue molar ellipticity $[\theta]_R$ (deg cm^2/dmol). The latter was divided by 10^3 and represented in the graphs as $[\theta]_R \times 10^{-3}$ (deg cm^2/dmol).

NMR spectroscopy of 10

Two-dimensional ^1H-NMR spectra were recorded in H_2O/D_2O (12:1, *v/v*) at 303 K. The peptide concentration was approximately 1 mM. The water signal was suppressed with 3-9-19 WATERGATE. The spin systems of all amino acid residues were identified using TOCSY spectra (mixing time of 80 ms and 12 ms) and additional phase-sensitive ^1H–^{13}C multiplicity-edited HSQC spectra. The sequence-specific assignment was accomplished using phase-sensitive ROESY spectra (mixing time of 200 ms). Spectra processing was carried out using TOPSPIN 3.2 from Bruker. The spectra were referenced to 4,4-dimethyl-4-silapentane-1-sulfonic acid (DSS) using the standard Bruker sample 2 mM sucrose/0.5 mM DSS at the same temperature and settings. ^{13}C chemical shifts were referenced using a scaling factor Ξ of 0.251449530 according to IUPAC recommendations [65]. Complete ^1H and ^{13}C resonance assignment was achieved using standard TOCSY, ROESY, and ^1H-^{13}C HSQC spectra (Table S2

and Figures S5 and S6). NOE distance restraints were derived from ROESY spectra. The NOE cross peaks were classified as very strong/medium strong/medium weak/weak corresponding to applied distance restraints of 2.5/3.5/4.5/5.5 Å.

Computational methods

Because of the available NOE constraints from NMR measurements, first, cyclopeptide **10** was built up using the protein builder and general builder functions of MOE2015.10 [63]. Afterwards, a series of restraints (Table S3) were applied for the given intramolecular distances on the basis of NMR measurements (H–H interactions) and the peptide was energy-minimized using the Amber 99 force field as implemented into MOE2015.10. This process led to the α-helical structure as presented in Figure 5. Subsequently, the restraints were lifted and the system was re-optimized. Upon optimization, the helical structure as well as the *trans*-configuration of the lactam bridge was preserved. All other cyclopeptides were generated starting from this structure by modifying or mutating the given residues. Subsequent optimization with the Amber 99 force field delivered the energy-minimized structures that were the starting point (one by one) for further molecular dynamics studies. To ensure full relaxation of the peptides in solution, we placed each one into a 35Å large cubic box of (explicit) water. The system was slowly heated up from 0 K to room temperature (RT) and then equilibrated at room temperature for 300 ps.

Cell viability assay

To determine the inhibitory effect of the cyclopeptide on cell viability, the MTT assay [66] was used. The human breast cancer cells T47D in Dulbecco's modified Eagle's medium containing 10% FBS and 1% penicillin–streptomycin were seeded into 96-well culture plates (1×10^4 cells per well). The day after, cells were treated with peptides at the concentrations of 50 μM and 500 μM in a medium containing 5% FBS as triplicates for 24 h. To determine the cell viability, 10 μl 5 mg/ml MTT solution were added to the peptide-treated and peptide-non-treated cells for 2 h at 37 °C in the dark. Then the medium was aspirated, cells were lysed with 100 μl DMSO, and the absorbance of the product formazan, which results from the reduction of MTT taking place only in the viable cells having an active metabolism, was measured at 550 nm with a Tecan Infinite M200 Pro microplate reader. Two independent experiments were performed (Figure S7).

Results and Discussion

Design and synthesis of the Lys-Asp-($i,i + 4$)-lactam-bridged peptides

To investigate whether the position of the Lys-Asp-($i,i + 4$)-lactam bridge may affect the conformation of the two octapeptide scaffolds, we designed three cyclic analogs based on junction-1 (**1–3**), in which the lactam bridge is at position (1,5), (2,6), or (3,7), and three cyclic analogs based on junction-2 (**4–6**), in which the lactam bridge is at position (2,6), (3,7), or (4,8) (Table 1). In the case of **3**, the (3,7)-lactam bridge would be adjacent to the C-terminal Pro, which might have additional effects on the conformation of the cyclic peptide; thus, we also designed an analog of **3** by replacing Pro with Ala (**7**). Additionally, to see whether the composition or sequence of the amino acid core triad ($i + 1,2,3$) might affect the conformation upon cyclization, we designed two

analogs of **3** and **7** by replacing their core triad KEL with KLE (**8** and **9**).

To further evaluate the role of the core triad on the conformation of a lactam-bridged peptide, we designed two series of cyclopeptides both based on junction-2 and with (2,6)-side chain cyclization (analogous to **4**), but containing RXQ (**10–14**) or QXQ (**15–17**) as core triad. The variable central residue X was Aib, Leu, norleucine (Nle), Trp, or Val. Finally, to distinguish the contribution of the core triad from that of the outer residues, we designed cyclopeptides **18** and **19**: Cyclopeptide **18** results from the combination of the core triad KEL of cyclopeptides **3** and **7** with the outer residues of cyclopeptides **4** and **10–16**. Cyclopeptide **19** contains the same outer residues as **18** but differs in the core triad, which is KEV instead of KEL.

The sequences were assembled on a Rink Amide MBHA resin by using Fmoc chemistry. The Lys and Asp side chains to be cyclized were protected with the Alloc and allyl groups, respectively, in order to allow the application of the on-resin cyclization strategy [67]. On-resin allyl/Alloc deprotection was performed by using Pd (PPh$_3$)$_4$ in the presence of PhSiH$_3$ [68], followed by cyclization with DEPBT/DIPEA. The HPLC and MS analysis of the crude products revealed different levels of success in the syntheses of the cyclopeptides: For example, attempts to cyclize the linear precursors of **2** and **6** failed, as the first was prone to dimerization, whereas the second remained mainly in the linear form. Moreover, in accordance with the high propensity of Asp(Oall) to form an aspartimide upon incorporation into a peptide chain, especially under basic conditions [69,70], we also observed the formation of an aspartimide during the assembly of some linear sequences, particularly of the linear precursors of cyclopeptides **7** and **9**, both containing the motif Asp(Oall)-Ala. Nevertheless, we were able to purify all cyclized peptides with a homogeneity ≥90%, with the exception of cyclopeptide **7**, whose homogeneity was ~70% (Figures S1–S3).

Effect of the lactam bridge position

The CD spectra of the two cyclic analogs of junction-1, **1** and **3**, are shown in Figure 2(A). The CD spectrum of **1**, in both water and water/TFE (70:30, *v/v*), is reminiscent of that of a 3$_{10}$-helix [71], with a negative band around 203 nm, a negative shoulder over the range 210–235 nm, and a positive signal below 195 nm. However, the weak mean residue ellipticity (between -2000 and -4000 deg cm^2/dmol) is indicative of the presence of turns. The CD spectrum of **3** in water displays a negative band at 200 nm but lacks any ellipticity above 210 nm. TFE has no significant effect on the CD signal above 210 nm, while it induces a detectable red shift (from 200 to 204 nm) and a decrease in intensity of the π–π* transition band. This excludes the presence of any helical motif in both water and water/TFE.

Based on the dichroic properties of cyclopeptides **1** and **3**, it is evident that none of them has the propensity to build an α-helical turn, despite the ($i,i + 4$)-side chain cyclization. The slightly different CD curves of **1** and **3** probably reflect different turn-type propensities as the result of the shift of the lactam bridge from the (1,5)-position to the (3,7)-position, the latter being immediately adjacent to the C-terminal Pro. In general, proline is a helix breaker and prefers positions at the extremities of a helix, in particular at N-cap + 1, N-cap − 1, and C-cap + 1 [72]. Alternatively, proline is often found at the corners of β-turns. In order to prove the effect of proline, we replaced Pro-8 in cyclopeptide **3** with Ala-8 and obtained cyclopeptide **7** that displays an α-helix-like CD curve in
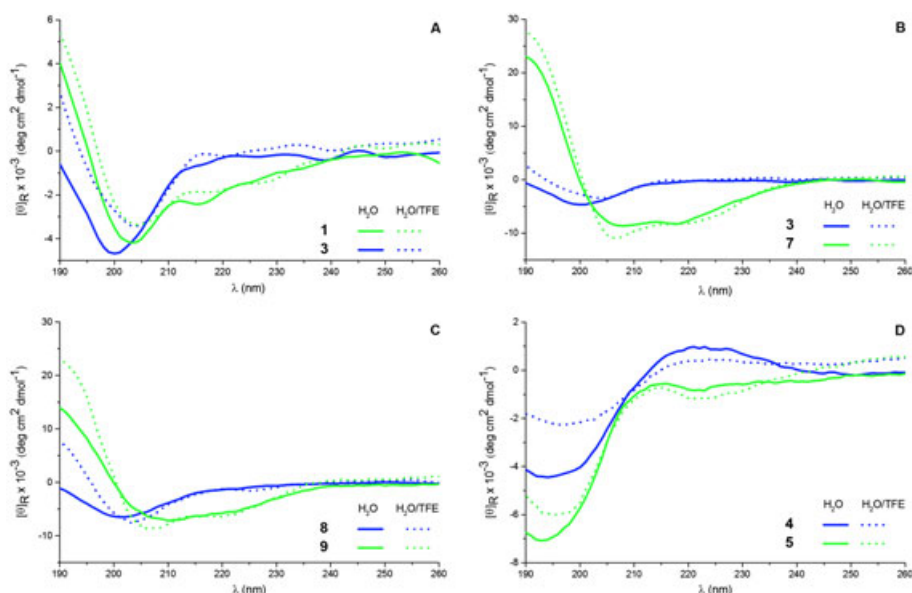
Figure 2. CD spectra of cyclopeptides **1**, **3–5**, and **7–9** in water and water/TFE (70:30, *v/v*). (A) Junction-1-derived cyclopeptides **1** (**K**RL**K**D**L**VP) and **3** (SR**K**KEL**D**P). (B,C) Effect of Pro/Ala at the (*i* + 5) position. Comparison of **3** (SR**K**KEL**D**P) with **7** (SR**K**KEL**D**A) (B) and of **8** (SR**K**KLE**D**P) with **9** (SR**K**KLE**D**A) (C). (D) Junction-2-derived cyclopeptides **4** (V**K**KVE**D**LQ) and **5** (VS**K**VEI**D**Q).

both water and water/TFE (Figure 2(B)). Similar behavior is shown by the Pro-8-containing cyclopeptide **8**, which is analogous to **3** but differs in the core sequence (KEL in **3** *versus* KLE in **8**), upon substitution of the C-terminal Pro-8 with Ala-8 (analog **9**) (Figure 2 (C)). Although the CD spectra of **7** and **9** are reminiscent of that of an α-helix, the fact that they show moderate mean residue ellipticity, especially of the two negative bands (less negative than $-10\,000$ deg cm^2/dmol), and are unaffected by the presence of TFE would suggest the formation of turns rather than of a helical motif.

The CD spectra of the two (2,6)-cyclized and (3,7)-cyclized analogs of junction-2, **4** and **5**, in water and in water/TFE, show a minimum below 200 nm and a weak band at 220–224 nm, which is positive for **4** and negative for **5** (Figure 2(D)). Addition of TFE to both peptides is accompanied by a positive ellipticity contribution to the CD signal below 200 nm and by a negative one around 220 nm. Again, the presence of any helical motif in these two cyclopeptides can be excluded in both water and water/TFE.

In summary, the dichroic properties of the two octapeptide scaffolds (junction-1/-2) upon (*i,i* + 4)-side chain cyclization lead to the following observations: (i) the constraint does not necessarily lead to the formation of an α-helical turn, while other turn types may be formed or still high flexibility may be maintained, and (ii) interestingly, TFE, which is known to favor the formation and stabilization of secondary structures, in particular the α-helix, has almost no effect on the cyclopeptides. This would suggest that they would lack the ability to build a canonical helical conformation.

Effect of the (*i* + 1,2,3) core residues

Based on the conformational properties of cyclopeptides **1**, **3–5**, and **7–9** and on the observations previously reported by Fairlie and coworkers [35], we attributed a role of the tripeptide motif included in the macrocycle (referred herein to as core triad) in determining the conformational properties of the macrolactam. Thus, we synthesized two series of cyclopeptides based on junction-2 and with (2,6)-side chain cyclization (analogous to
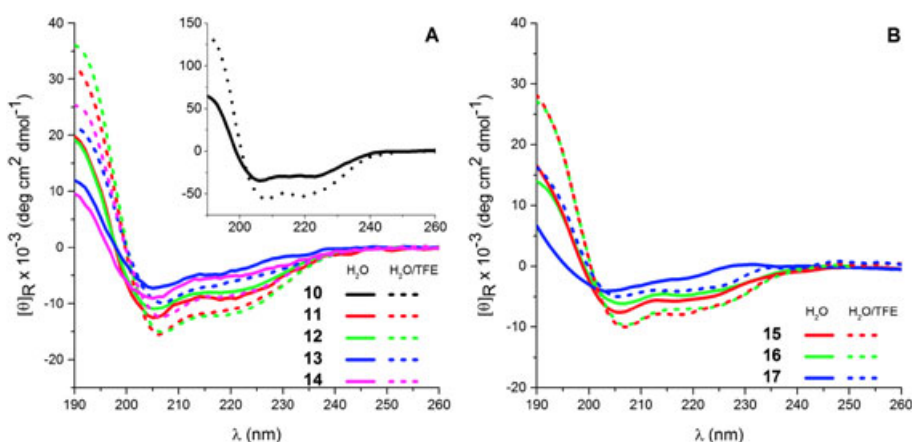

Figure 3. CD spectra of the junction-2-derived cyclopeptides **10–14** and **15–17** in water and water/TFE (70:30, *v/v*). (A) **10–14** (V**K**RXQ**D**LQ: X = Aib (**10**), Leu (**11**), Nle (**12**), Trp (**13**), Val (**14**)). (B) **15–17** (V**K**QXQ**D**LQ: X = Leu (**15**), Nle (**16**), Trp (**17**)).

cyclopeptide **4**), but differing in their core triad, which was RXQ for peptides **10**–**14** and QXQ for peptides **15**–**17** (X = Aib, Leu, Nle, Trp, Val).

With the exception of **17**, all cyclopeptides are characterized by helix-like CD spectra (Figure 3). Moreover, in contrast to the cyclopeptides with no helix-like CD signature described earlier (Figure 2), their conformation is positively affected by the presence of TFE, suggesting the stabilization of an α-helical motif. The CD intensity decreases in the order of **10** (X = Aib) $\gg$ **11** (X = Leu) ~ **12** (X = Nle) > **13** (X = Trp) ~ **14** (X = Val), which reflects the decreasing intrinsic helix propensity of the residue at position X. Indeed, Aib is a well-known α-helix and 3_{10}-helix stabilizer [39], and Leu is reported to be more helix-prone than Trp and Val of about 0.3–0.4 kcal/mol [73]. Based on our CD data, Nle seems to have helical propensity comparable with Leu (**11** versus **12** or **15** versus **16**).
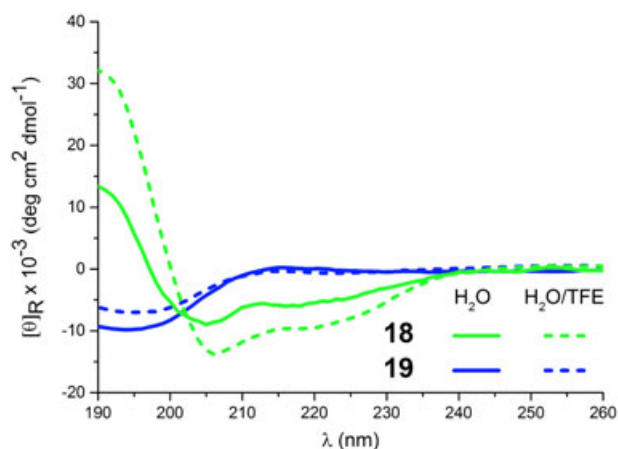

Figure 4. CD spectra of cyclopeptides **18** (V**K**KEL**D**LQ) and **19** (V**K**KEV**D**LQ) in water and water/TFE (70:30, v/v).

The CD spectra of the cyclopeptides containing the core triad RXQ are more intense than those of the cyclopeptides containing the core triad QXQ. This would be in accordance with the superior helix propensity of Arg over Gln of about 0.2 kcal/mol [73]. In addition, the loss of the positive charge of Arg was found to negatively affect the solubility of the cyclopeptides, likely because of peptide aggregation, particularly in the case of the Trp-containing cyclopeptide **17**. The latter displays a CD curve in water, which clearly differs from those of the other cyclopeptides shown in Figure 3. Moreover, the effect of TFE on the CD intensity is not as strong as in the case of the other cyclopeptides, suggesting that the formation of an α-helical motif is less favored.

In summary, the intrinsic secondary structure propensity of the residues in the macrolactam seems to influence the conformational preferences of the (2,6)-cyclized peptides, in agreement with the results by Fairlie and coworkers [35]: Indeed, the α-helical propensity of the cyclopeptides increased with the increasing intrinsic helix propensity of the core triad.

Effect of the outer residues other than proline

The different conformational properties between cyclopeptide **4** (non-helix-like and TFE-insensitive CD signature) and cyclopeptides **10**–**16** (helix-like and TFE-sensitive CD signature), which share the same outer residues (N-terminal Val and C-terminal Leu-Gln) but have a different core triad, would suggest a major structural role of the core triad rather than of the outer residues. However, we showed that the presence of Pro rather than Ala at position (i + 5) significantly affects the structure of the (3,7)-lactam-bridged peptides. This suggests that also the outer residues may contribute to the conformation adopted by the macrocycle. In order to compare the different impacts of the core and outer residues on the cyclopeptide conformation, we prepared cyclopeptide **18**, which results from the combination of the core triad (KEL) of
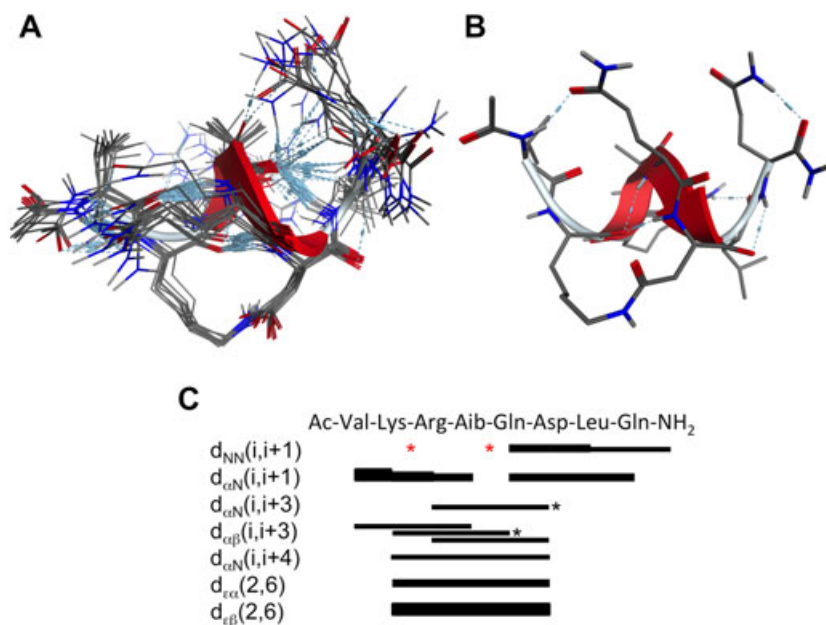

Figure 5. NMR-derived structure of the Aib-containing cyclopeptide **10** in water. (A) Superposition of ten lowest-energy structures from the molecular dynamics simulation. (B) View of one of the ten lowest-energy structures shown in (A). (C) NOE summary diagram (the NOE cross peaks were classified as very strong/medium strong/medium weak/weak corresponding to the upper distance restraints 2.5/3.5/4.5/5.5 Å, which are indicated by the thickness of the bars. Black asterisks indicate NOE signals with overlap; red asterisks indicate NOE signals that would lie on the diagonal).
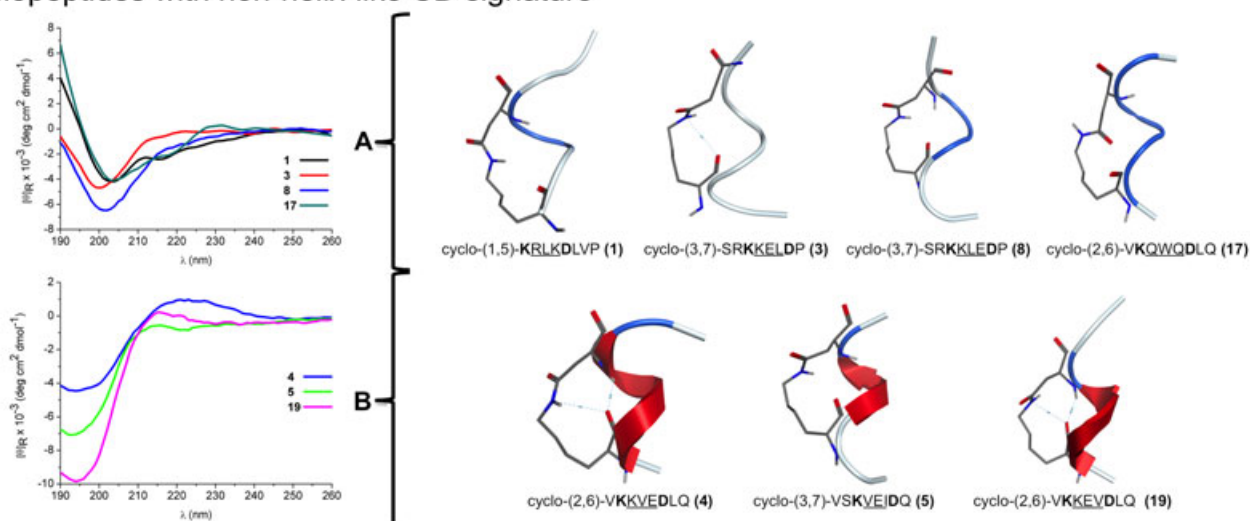
cyclopeptide **7**, which is characterized by a helix-like but TFE-unaffected CD signature, and the outer residues (N-terminal Val and C-terminal Leu-Gln) of cyclopeptides **4** (non-helix-like and TFE-insensitive CD signature) and **10**–**16** (helix-like and TFE-sensitive CD signature). The CD signature of **18** remains helix like; however, contrarily to that of cyclopeptide **7**, it is affected by TFE (Figure 4), similar to the cyclopeptides **10**–**16** (Figure 3). This confirms that also the outer residues contribute to the overall conformation of the lactam-bridged peptide. Nevertheless, the most important conformational contribution seems to come from the residues forming the skeleton of the macrolactam: Indeed, an analog of **18**, in which the core triad KEL was replaced with KEV (**19**), does not

show an α-helix-like CD signature (Figure 4), but rather a CD curve similar to that found for cyclopeptides **4** and **5** (Figure 2(D)).
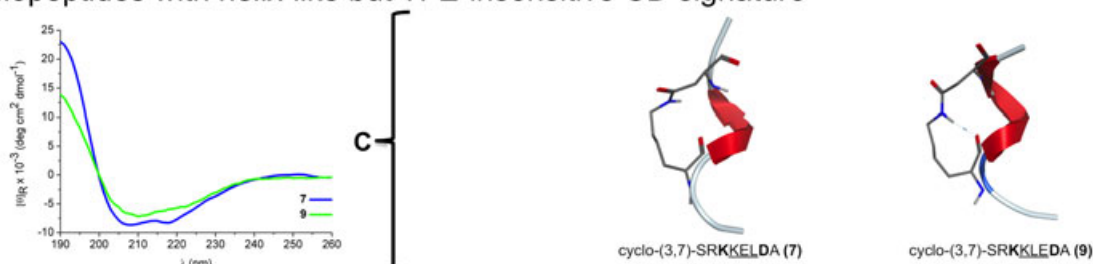
Computed structures of the cyclopeptides

We used computational methods to assess the intrinsic ability of the cyclopeptides to adopt a helical conformation, starting from the NMR-derived helical structure of the Aib-containing cyclopeptide (**10**), which is shown in Figure 5. This helical structure is stabilized by two (i–i + 3/4) H-bonds (Lys-2-CO-Gln-5/Asp-6-NH and Arg-3-CO-Asp-6/Leu-7-NH).
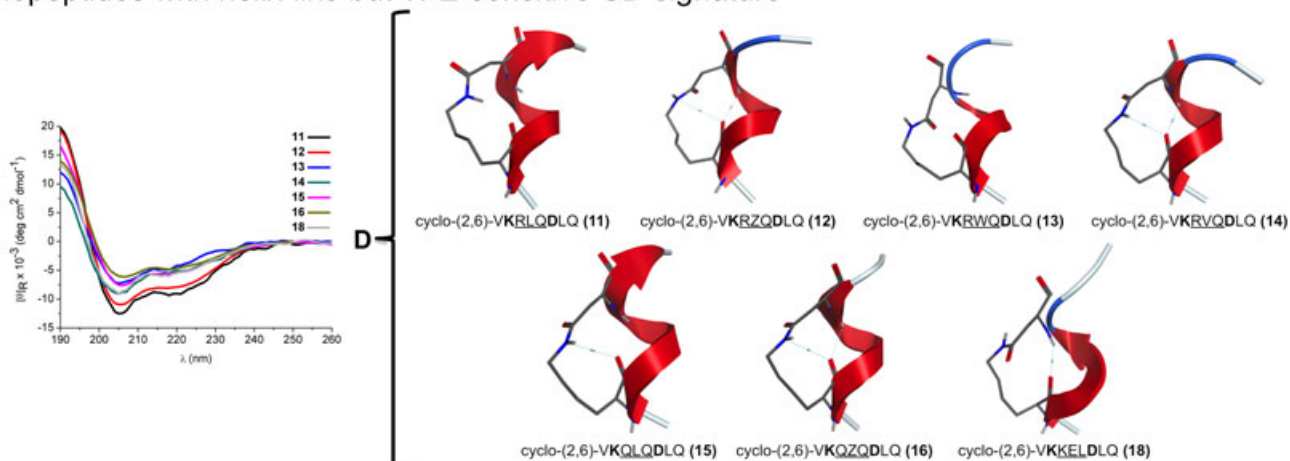

Figure 6. Computed structures of the cyclopeptides based on the NMR-derived helical structure of cyclopeptide **10**.

In general, the computed structures are in agreement with the CD spectra. Indeed, cyclopeptides **1**, **3**, **8**, and **17**, for which not well-defined conformations were obtained by the computational approach (Figure 6), all show a similar but non-helix-like CD signature (group A), with the exception of **1** and **17**, which are reminiscent of the 3_{10}-helix CD signature, albeit with low intensity. In contrast, in the case of cyclopeptides **4**, **5**, and **19**, which are all characterized by a non-helix-like CD signature with a negative band below 200 nm (group B), secondary structure elements are formed during the molecular dynamics simulation. Cyclopeptide **4** seems even to be able to build a helical conformation, but its CD curve rather suggests the absence of a canonical α-helix motif.

The helix-like but TFE-insensitive CD signature of the two cyclic peptides **7** and **9** (group C) may reflect their computed structures that show a partially ordered backbone conformation. Finally, cyclopeptides **11**–**16** and **18**, which all show helix-like and TFE-sensitive CD curves (group D), also display computed structures with a well-defined helical backbone conformation.

Conclusions

By preparing and characterizing a series of octapeptides containing a Lys-Asp-($i,i + 4$)-lactam bridge, we observed a strong impact of the primary structure on the conformational properties of the peptide-based macrolactams. For the Lys-Asp-(2,6)-cyclopeptide scaffold containing no proline, we found that the CD signature was dependent on the core triad. However, also the role of the flanking residues cannot be neglected: For example, the combination of the core triad KEL with different outer residues like in **3**, **7**, and **18** led to three different CD signatures, with only **18** displaying a helix-like and TFE-sensitive CD curve. The results of the computational studies on the cyclopeptides were generally in agreement with the corresponding CD signatures. Moreover, with the exception of the cyclopeptide series containing the core triads RXQ or QXQ (**10**–**17**), no clear correlation between primary structure and helix structure propensity could be identified. Probably, the overall dynamics of the cyclic structure (at both the backbone and side chain level) determines the formation and stabilization of a well-defined conformation.

Intermolecular interactions require specific spatial arrangements of the amino acid side chains, which are either presented by well-defined structures or may be built by an induced fit mechanism, as in the case of intrinsically disordered proteins involving helical secondary structures [74–77]. Obviously, increasing the conformational rigidity of a peptide may favor molecular recognition events, provided that the spatial arrangement of the groups involved in the recognition is suitable. We will investigate in the near future whether the introduction of a constraint in the form of a lactam bridge in a peptide ligand candidate may be of benefit for the molecular recognition of the Id proteins and for their inhibition in cells. A preliminary screening has been carried out to evaluate the ability of cyclopeptides **5** (group B), **10**–**16** and **18** (group D), and **17** (group A) to decrease the viability of a breast adenocarcinoma cell line (T47D) that displays dysregulated Id protein activity in the presence of serum or growth factors [78]; indeed, the Id proteins are known to promote cell proliferation [79–81]. At the concentration of 500 μM, all peptides decreased cell viability to about 50%, with the exception of the Aib-4-containing peptide **10** and the Trp-4-containing peptides **13** and **17** (Figure S7). Interestingly, **5**, **12**, and **18** induced the same cell response already at a concentration of 50 μM. It should be noted that **5**,

unlike **12** and **18**, was characterized by a non-helix-like CD signature. These data would suggest that the helical content of the ligand is not sufficient to induce a cellular response: Indeed, **10** and **13** possess higher helical content than **5**, but contrarily to the latter, they had no effect on the cells. This might be due to an unfavorable interaction pattern displayed by the cyclopeptide (Figure S7) or to a loss of conformational dynamics: In this regard, it has been recently reported that the highly rigid three-disulfide-bonded scyllatoxin was not suitable for protein grafting and Bcl-2 protein targeting; however, its reduced form was, suggesting the importance of induced fit mechanisms in binding to the Bcl-2 protein [82].

Besides (and as a result of) structural rigidity, peptide constraints may affect other properties of the peptide itself like solubility and self-assembly propensity. Very recently, the impact of Aib on the aggregation behavior of peptides has been discussed [83]: in particular, it has been pointed out that Aib may stabilize the helical conformation of a peptide and, in turn, trigger the formation of highly ordered self-assembled structures. This suggests that, besides biological, structural, and pharmacokinetic/dynamic properties, also biophysical properties (particularly aggregation) should be taken into account to fully characterize constrained peptides.

References

1 Ali MH, Imperiali B. Protein oligomerization: how and why. *Bioorg. Med. Chem.* 2005; **13**: 5013–5020.
2 Braun P, Gingras AC. History of protein–protein interactions: from egg-white to complex networks. *Proteomics* 2012; **12**: 1478–1498.
3 Cabrele C, Martinek TA, Reiser O, Berlicki L. Peptides containing beta-amino acid patterns: challenges and successes in medicinal chemistry. *J. Med. Chem.* 2014; **57**: 9718–9739.
4 Checco JW, Kreitler DF, Thomas NC, Belair DG, Rettko NJ, Murphy WL, Forest KT, Gellman SH. Targeting diverse protein-protein interaction interfaces with alpha/beta-peptides derived from the z-domain scaffold. *Proc. Natl. Acad. Sci. U. S. A.* 2015a; **112**: 4552–4557.
5 Checco JW, Lee EF, Evangelista M, Sleebs NJ, Rogers K, Pettikiriarachchi A, Kershaw NJ, Eddinger GA, Belair DG, Wilson JL, Eller CH, Raines RT, Murphy WL, Smith BJ, Gellman SH, Fairlie WD. Alpha/beta-peptide foldamers targeting intracellular protein–protein interactions with activity in living cells. *J. Am. Chem. Soc.* 2015b; **137**: 11365–11375.
6 Grison CM, Miles JA, Robin S, Wilson AJ, Aitken DJ. An α-helix-mimicking 12,13-helix: designed α/β/γ-foldamers as selective inhibitors of protein–protein interactions. *Angew. Chem. Int. Ed.* 2016; **55**: 11096–11100.
7 Hilinski GJ, Kim YW, Hong J, Kutchukian PS, Crenshaw CM, Berkovitch SS, Chang A, Ham S, Verdine GL. Stitched alpha-helical peptides via bis ring-closing metathesis. *J. Am. Chem. Soc.* 2014; **136**: 12314–12322.
8 Sawada T, Gellman SH. Structural mimicry of the alpha-helix in aqueous solution with an isoatomic alpha/beta/gamma-peptide backbone. *J. Am. Chem. Soc.* 2011; **133**: 7336–7339.
9 Shim SY, Kim YW, Verdine GL. A new i, i+3 peptide stapling system for alpha-helix stabilization. *Chem. Biol. Drug Des.* 2013; **82**: 635–642.
10 Verdine GL, Hilinski GJ. Stapled peptides for intracellular drug targets. *Methods Enzymol.* 2012; **503**: 3–33.
11 Werner HM, Horne WS. Folding and function in alpha/beta-peptides: targets and therapeutic applications. *Curr. Opin. Chem. Biol.* 2015; **28**: 75–82.
12 Ghadiri MR, Choi C. Secondary structure nucleation in peptides. Transition metal ion stabilized alpha-helices. *J. Am. Chem. Soc.* 1990; **112**: 1630–1632.

13 Ruan F, Chen Y, Hopkins PB. Metal ion-enhanced helicity in synthetic peptides containing unnatural, metal-ligating residues. *J. Am. Chem. Soc.* 1990; **112**: 9403–9404.

14 Kemp DS, Curran TP, Boyd JG, Allen TJ. Studies of n-terminal templates for alpha-helix formation. Synthesis and conformational analysis of peptide conjugates of (2s,5s,8s,11s)-1-acetyl-1,4-diaza-3-keto-5-carboxy-10-thiatricyclo[2.8.1.04,8]tridecane (ac-hel1-oh). *J. Org. Chem.* 1991; **56**: 6683–6697.

15 Lewis AJ, Rutherford T, Wilkie J, Jenn T, Gani D. Design, construction and properties of peptide n-terminal cap templates devised to initiate [small alpha]-helices. Part 3. Caps derived from n-[(2s)-2-chloropropionyl]-(2s)-pro-(2r)-ala-(2s,4s)-4-thiopro-ome. *J. Chem. Soc. Perkin Trans.* 1998a; **1**: 3795–3806.

16 Lewis A, Wilkie JJ, Rutherford T, Gani D. Design, construction and properties of peptide n-terminal cap templates devised to initiate [small alpha]-helices. Part 2. Caps derived from n-[(2s)-2-chloropropionyl]-(2s)-pro-(2s)-pro-(2s,4s)-4-thiopro-ome. *J. Chem. Soc. Perkin Trans.* 1998b; **1**: 3777–3794.

17 Cabezas E, Satterthwait AC. The hydrogen bond mimic approach: solid-phase synthesis of a peptide stabilized as an α-helix with a hydrazone link. *J. Am. Chem. Soc.* 1999; **121**: 3862–3875.

18 Henchey LK, Kushal S, Dubey R, Chapman RN, Olenyuk BZ, Arora PS. Inhibition of hypoxia inducible factor 1-transcription coactivator interaction by a hydrogen bond surrogate α-helix. *J. Am. Chem. Soc.* 2009; **132**: 941–943.

19 Albert JS, Hamilton AD. Stabilization of helical domains in short peptides using hydrophobic interactions. *Biochemistry* 1995; **34**: 984–990.

20 Mayne L, Englander SW, Qiu R, Yang J, Gong Y, Spek EJ, Kallenbach NR. Stabilizing effect of a multiple salt bridge in a prenucleated peptide. *J. Am. Chem. Soc.* 1998; **120**: 10643–10645.

21 Jackson DY, King DS, Chmielewski J, Singh S, Schultz PG. General approach to the synthesis of short alpha-helical peptides. *J. Am. Chem. Soc.* 1991; **113**: 9391–9392.

22 Diderich P, Bertoldo D, Dessen P, Khan MM, Pizzitola I, Held W, Huelsken J, Heinis C. Phage selection of chemically stabilized alpha-helical peptide ligands. *ACS Chem. Biol.* 2016; **11**: 1422.

23 Hu K, Geng H, Zhang Q, Liu Q, Xie M, Sun C, Li W, Lin H, Jiang F, Wang T, Wu Y-D, Li Z. An in-tether chiral center modulates the helicity, cell permeability, and target binding affinity of a peptide. *Angew. Chem. Int. Ed.* 2016; **55**: 8013–8017.

24 Cantel S, Halperin JA, Chorev M, Scrima M, D'Ursi AM, Levy JJ, DiMarchi RD, Le Chevalier A, Rovero P, Papini AM. Side chain-to-side chain cyclization by intramolecular click reaction-building blocks, solid phase synthesis and conformational characterization. *Adv. Exp. Med. Biol.* 2009; **611**: 175–176.

25 Cantel S, Isaad Ale C, Scrima M, Levy JJ, DiMarchi RD, Rovero P, Halperin JA, D'Ursi AM, Papini AM, Chorev M. Synthesis and conformational analysis of a cyclic peptide obtained via i to i+4 intramolecular side-chain to side-chain azide-alkyne 1,3-dipolar cycloaddition. *J. Org. Chem.* 2008; **73**: 5663–5674.

26 Blackwell HE, Sadowsky JD, Howard RJ, Sampson JN, Chao JA, Steinmetz WE, O'Leary DJ, Grubbs RH. Ring-closing metathesis of olefinic peptides: design, synthesis, and structural characterization of macrocyclic helical peptides. *J. Org. Chem.* 2001; **66**: 5291–5302.

27 Kim YW, Kutchukian PS, Verdine GL. Introduction of all-hydrocarbon i,i+3 staples into alpha-helices via ring-closing olefin metathesis. *Org. Lett.* 2010; **12**: 3046–3049.

28 Schafmeister CE, Po J, Verdine GL. An all-hydrocarbon cross-linking system for enhancing the helicity and metabolic stability of peptides. *J. Am. Chem. Soc.* 2000; **122**: 5891–5892.

29 Caporale A, Sturlese M, Gesiot L, Zanta F, Wittelsberger A, Cabrele C. Side chain cyclization based on serine residues: synthesis, structure, and activity of a novel cyclic analogue of the parathyroid hormone fragment 1-11. *J. Med. Chem.* 2010; **53**: 8072–8079.

30 Bracken C, Gulyas J, Taylor JW, Baum J. Synthesis and nuclear magnetic resonance structure determination of an alpha-helical, bicyclic, lactam-bridged hexapeptide. *J. Am. Chem. Soc.* 1994; **116**: 6431–6432.

31 Osapay G, Taylor JW. Multicyclic polypeptide model compounds. 1. Synthesis of a tricyclic amphiphilic alpha-helical peptide using an oxime resin, segment-condensation approach. *J. Am. Chem. Soc.* 1990; **112**: 6046–6051.

32 Osapay G, Taylor JW. Multicyclic polypeptide model compounds. 2. Synthesis and conformational properties of a highly alpha-helical uncosapeptide constrained by three side-chain to side-chain lactam bridges. *J. Am. Chem. Soc.* 1992; **114**: 6966–6973.

33 Phelan JC, Skelton NJ, Braisted AC, McDowell RS. A general method for constraining short peptides to an α-helical conformation. *J. Am. Chem. Soc.* 1997; **119**: 455–460.

34 Schievano E, Mammi S, Bisello A, Rosenblatt M, Chorev M, Peggion E. Conformational studies of a bicyclic, lactam-constrained parathyroid hormone-related protein-derived agonist. *J. Pept. Sci.* 1999; **5**: 330–337.

35 Shepherd NE, Hoang HN, Abbenante G, Fairlie DP. Single turn peptide alpha helices with exceptional stability in water. *J. Am. Chem. Soc.* 2005; **127**: 2974–2983.

36 Shepherd NE, Hoang HN, Desai VS, Letouze E, Young PR, Fairlie DP. Modular α-helical mimetics with antiviral activity against respiratory syncytial virus. *J. Am. Chem. Soc.* 2006; **128**: 13284–13289.

37 Taylor JW. The synthesis and study of side-chain lactam-bridged peptides. *Biopolymers (Pept. Sci.)* 2002; **66**: 49–75.

38 Yu C, Taylor JW. Synthesis and study of peptides with semirigid i and i+7 side-chain bridges designed for α-helix stabilization. *Bioorg. Med. Chem.* 1999; **7**: 161–175.

39 Karle IL, Balaram P. Structural characteristics of alpha-helical peptide molecules containing aib residues. *Biochemistry* 1990; **29**: 6747–6756.

40 Carpenter KA, Schmidt R, Yue SY, Hodzic L, Pou C, Payza K, Godbout C, Brown W, Roberts E. The glycine-1 residue in cyclic lactam analogues of galanin(1–16)-NH2 is important for stabilizing an n-terminal helix. *Biochemistry* 1999; **38**: 15295–15304.

41 Geistlinger TR, Guy RK. An inhibitor of the interaction of thyroid hormone receptor β and glucocorticoid interacting protein 1. *J. Am. Chem. Soc.* 2001; **123**: 1525–1526.

42 Tsomaia N, Pellegrini M, Hyde K, Gardella TJ, Mierke DF. Toward parathyroid hormone minimization: conformational studies of cyclic PTH(1−14) analogues. *Biochemistry* 2004; **43**: 690–699.

43 Lasorella A, Benezra R, Iavarone A. The ID proteins: master regulators of cancer stem cells and tumour aggressiveness. *Nat. Rev. Cancer* 2014; **14**: 77–91.

44 Norton JD. ID helix–loop–helix proteins in cell growth, differentiation and tumorigenesis. *J. Cell Sci.* 2000; **113**: 3897–3905.

45 Perk J, Iavarone A, Benezra R. Id family of helix–loop–helix proteins in cancer. *Nat. Rev. Cancer* 2005; **5**: 603–614.

46 Ruzinova MB, Benezra R. Id proteins in development, cell cycle and cancer. *Trends Cell Biol.* 2003; **13**: 410–418.

47 Langlands K, Yin X, Anand G, Prochownik EV. Differential interactions of ID proteins with basic-helix–loop–helix transcription factors. *J. Biol. Chem.* 1997; **272**: 19785–19793.

48 Massari ME, Murre C. Helix–loop–helix proteins: regulators of transcription in eucaryotic organisms. *Mol. Cell. Biol.* 2000; **20**: 429–440.

49 Sun XH, Copeland NG, Jenkins NA, Baltimore D. Id proteins Id1 and Id2 selectively inhibit DNA binding by one class of helix–loop–helix proteins. *Mol. Cell. Biol.* 1991; **11**: 5603–5611.

50 Sikder HA, Devlin MK, Dunlap S, Ryu B, Alani RM. Id proteins in cell growth and tumorigenesis. *Cancer Cell* 2003; **3**: 525–530.

51 Alani RM, Young AZ, Shifflett CB. Id1 regulation of cellular senescence through transcriptional repression of p16/ink4a. *Proc. Natl. Acad. Sci. U. S. A.* 2001; **98**: 7812–7816.

52 Garland W, Benezra R, Chaudhary J. Targeting protein–protein interactions to treat cancer-recent progress and future directions. *Annu. Rep. Med. Chem.* 2013; **48**: 227–245.

53 Roschger C, Cabrele C. The Id-protein family in developmental and cancer-associated pathways. *Cell Commun. Signal* 2017; **15**: 7. https://doi.org/10.1186/s12964-12016-10161-y

54 Chen CH, Kuo SC, Huang LJ, Hsu MH, Lung FD. Affinity of synthetic peptide fragments of myod for Id1 protein and their biological effects in several cancer cells. *J. Pept. Sci.* 2010; **16**: 231–241.

55 Pellegrino S, Ferri N, Colombo N, Cremona E, Corsini A, Fanelli R, Gelmi ML, Cabrele C. Synthetic peptides containing a conserved sequence motif of the Id protein family modulate vascular smooth muscle cell phenotype. *Bioorg. Med. Chem. Lett.* 2009; **19**: 6298–6302.

56 Beisswenger M, Cabrele C. Self-recognition behavior of a helix–loop–helix domain by a fragment scan. *Biochim. Biophys. Acta* 1844; **2014**: 1675–1683.

57 Eletsky A, Wang, D, Kohan, E, Janjua, H, Acton, TB, Xiao, R, Everett, JK, Montelione, GT, Szyperski, T, Solution NMR structure of the helix–loop–helix domain of human ID3 protein, northeast structural genomics consortium target Hr3111a. 2011; 10.2210/pdb2lfh/pdb.

58 Wong MV, Jiang S, Palasingam P, Kolatkar PR. A divalent ion is crucial in the structure and dominant-negative function of ID proteins, a class of helix–loop–helix transcription regulators. *PLoS One* 2012; **7**: e48591.

59 Beisswenger M, Yoshiya T, Kiso Y, Cabrele C. Synthesis and conformation of an analog of the helix–loop–helix domain of the Id1 protein containing the O-acyl iso-prolyl-seryl switch motif. *J. Pept. Sci.* 2010; **16**: 303–308.

60 Kiewitz SD, Cabrele C. Synthesis and conformational properties of protein fragments based on the Id family of DNA-binding and cell-differentiation inhibitors. *Biopolymers (Pept. Sci.)* 2005; **80**: 762–774.

61 Kiewitz SD, Kakizawa T, Kiso Y, Cabrele C. Switching from the unfolded to the folded state of the helix–loop–helix domain of the Id proteins based on the O-acyl isopeptide method. *J. Pept. Sci.* 2008; **14**: 1209–1215.

62 Toniolo C, Crisma M, Formaggio F, Peggion C. Control of peptide conformation by the Thorpe–Ingold effect (C-alpha-tetrasubstitution). *Biopolymers* 2001; **60**: 396–419.

63 Molecular Operating Environment (MOE), Chemical Computing Group Inc., 1010 Sherbooke St. West, Suite #910, Montreal, QC, Canada, H3A 2R7 2016.

64 Valiev M, Bylaska EJ, Govind N, Kowalski K, Straatsma TP, van Dam HJJ, Wang D, Nieplocha J, Apra E, Windus TL, de Jong WA. NWChem: a comprehensive and scalable open-source solution for large scale molecular simulations. *Comput. Phys. Commun.* 2010; **181**: 1477–1489.

65 Markley JL, Bax A, Arata Y, Hilbers CW, Kaptein R, Sykes BD, Wright PE, Wüthrich K. Recommendations for the presentation of NMR structures of proteins and nucleic acids. *Pure Appl. Chem.* 1988; **70**: 117–142.

66 Mosmann T. Rapid colorimetric assay for cellular growth and survival: application to proliferation and cytotoxicity assays. *J. Immunol. Methods* 1983; **65**: 55–63.

67 Grieco P, Gitu PM, Hruby VJ. Preparation of 'side-chain-to-side-chain' cyclic peptides by allyl and Alloc strategy: potential for library synthesis. *J. Pept. Res.* 2001; **57**: 250–256.

68 Guibé F. Allylic protecting groups and their use in a complex environment. Part ii: allylic protecting groups and their removal through catalytic palladium π-allyl methodology. *Tetrahedron* 1998; **54**: 2967–3042.

69 Kunz H, Waldmann H, Unverzagt C. Allyl ester as temporary protecting group for the β-carboxy function of aspartic acid. *Int. J. Pept. Protein Res.* 1985; **26**: 493–497.

70 Vigil-Cruz SC, Aldrich JV. Unexpected aspartimide formation during coupling reactions using Asp(OAl) in solid-phase peptide synthesis. *Lett. Pept. Sci.* 1999; **6**: 71–75.

71 Toniolo C, Formaggio F, Tognon S, Broxterman QB, Kaptein B, Huang R, Setnicka V, Keiderling TA, McColl IH, Hecht L, Barron LD. The complete chirospectroscopic signature of the peptide 3(10)-helix in aqueous solution. *Biopolymers* 2004; **75**: 32–45.

72 Kim MK, Kang YK. Positional preference of proline in alpha-helices. *Protein Sci.* 1999; **8**: 1492–1499.

73 Pace CN, Scholtz JM. A helix propensity scale based on experimental studies of peptides and proteins. *Biophys. J.* 1998; **75**: 422–427.

74 Perkins JR, Diboun I, Dessailly BH, Lees JG, Orengo C. Transient protein–protein interactions: structural, functional, and network properties. *Structure* 2010; **18**: 1233–1243.

75 Rogers JM, Steward A, Clarke J. Folding and binding of an intrinsically disordered protein: fast, but not 'diffusion-limited'. *J. Am. Chem. Soc.* 2013; **135**: 1415–1422.

76 Rogers JM, Wong CT, Clarke J. Coupled folding and binding of the disordered protein PUMA does not require particular residual structure. *J. Am. Chem. Soc.* 2014; **136**: 5197–5200.

77 Shammas SL, Travis AJ, Clarke J. Remarkably fast coupled folding and binding of the intrinsically disordered transactivation domain of cMyb to CBP KIX. *J. Phys. Chem. B* 2013; **117**: 13346–13356.

78 Fong S, Itahana Y, Sumida T, Singh J, Coppe JP, Liu Y, Richards PC, Bennington JL, Lee NM, Debs RJ, Desprez PY. Id-1 as a molecular target in therapy for breast cancer cell invasion and metastasis. *Proc. Natl. Acad. Sci. U. S. A.* 2003; **100**: 13543–13548.

79 Iavarone A, Garg P, Lasorella A, Hsu J, Israel MA. The helix–loop–helix protein Id-2 enhances cell proliferation and binds to the retinoblastoma protein. *Genes Dev.* 1994; **8**: 1270–1284.

80 Jung S, Park RH, Kim S, Jeon YJ, Ham DS, Jung MY, Kim SS, Lee YD, Park CH, Suh-Kim H. Id proteins facilitate self-renewal and proliferation of neural stem cells. *Stem Cells Dev.* 2010; **19**: 831–841.

81 Lasorella A, Rothschild G, Yokota Y, Russell RG, Iavarone A. Id2 mediates tumor initiation, proliferation, and angiogenesis in rb mutant mice. *Mol. Cell. Biol.* 2005; **25**: 3563–3574.

82 Harris MM, Coon Z, Alqaeisoom N, Swords B, Holub JM. Targeting anti-apoptotic Bcl2 proteins with scyllatoxin-based BH3 domain mimetics. *Org. Biomol. Chem.* 2016; **14**: 440–446.

83 Venanzi M, Gatto E, Formaggio F, Toniolo C. The importance of being Aib. Aggregation and self-assembly studies on conformationally constrained oligopeptides. *J. Pept. Sci.* 2017; **23**: 104–116.

Supporting information

Additional Supporting Information may be found online in the supporting information tab for this article.